REPORT DOCUMENTATION

AD-A257 077

1. AGENCY USE ONLY (Leave blank)	2. REPORT DATE
	OCTOBER, 1992

4. TITLE AND SUBTITLE
SOLVENT DYNAMICAL EFFECTS IN ELECTRON TRANSFER: ELECTROCHEMICAL-EXCHANGE KINETICS OF SESQUIBICYCLIC HYDRAZINES AS A PROBE OF COUPLED VIBRATIONAL ACTIVATION

5. FUNDING NUMBERS
CONTRACT NO.
N00014-91-J-1409

6 AUTHOR(S)
DONALD K. PHELPS, MICHAEL T. RAMM, YICHUN WANG, STEPHEN F. NELSEN AND MICHAEL J. WEAVER

7. PERFORMING ORGANIZATION NAME(S) AND ADDRESS(ES)
PURDUE UNIVERSITY
DEPARTMENT OF CHEMISTRY
1393 BROWN BUILDING
WEST LAFAYETTE, INDIANA 47903-1393

8. PERFORMING ORGANIZATION REPORT NUMBER
TECHNICAL REPORT NO. 132

9 SPONSORING/MONITORING AGENCY NAME(S) AND ADDRESS(ES)
DIVISION OF SPONSORED PROGRAMS
PURDUE RESEARCH FOUNDATION
PURDUE UNIVERISTY
WEST LAFAYETTE, INDIANA 47907

10. SPONSORING/MONITORING AGENCY REPORT NUMBER

11. SUPPLEMENTARY NOTES

12a. DISTRIBUTION/AVAILABILITY STATEMENT
APPROVED FOR PUBLIC RELEASE AND SALE; ITS DISTRIBUTION IS UNLIMITED

12b. DISTRIBUTION CODE

13. ABSTRACT (Maximum 200 words)

Rate constants for electrochemical exchange of three sesquibicyclic hydrazine-radical cation redox couples, k°_{ex}, obtained at mercury by means of phase-selective ac voltammetry, are reported in seven solvents - acetonitrile, acetone, nitromethane, N, N-dimethylformamide, dimethylsulfoxide, benzonitrile and methanol. The hydrazine couples - denoted here $1^{+/0}$, $2^{+/0}$, and $3^{+/0}$ - feature variations in the bridgehead alkyl groups; they each exhibit substantial high-frequency vibrational barriers (4.5-5 kcal mol^{-1}) to electrochemical exchange. These systems therefore provide an interesting opportunity for the assessment of the manner and extent in which overdamped solvent relaxation may limit the electron-transfer dynamics under such circumstances. As in previous studies (ref. 2), scrutiny of the solvent-dependent rate constants enable at least semiquantitative estimates of the degree to which the kinetics are controlled by solvent dynamics as well as activation energetics. In addition to the usual dielectric-continuum treatment, estimates of the latter outer-shell component required for the solvent-dynamical analysis were required from an observed

14 SUBJECT TERMS	15. NUMBER OF PAGES
SESQUIBICYCLIC HYDRAZINES, ELECTRON-TRANSFER DYNAMICS, ELECTROCHEMICAL-EXCHANGE KINETICS	37
	16. PRICE CODE

17. SECURITY CLASSIFICATION OF REPORT	18. SECURITY CLASSIFICATION OF THIS PAGE	19. SECURITY CLASSIFICATION OF ABSTRACT	20. LIMITATION OF ABSTRACT
UNCLASSIFIED	UNCLASSIFIED	UNCLASSIFIED	UL

13. ABSTRACT (continued)

correlation between rates of $1^{+/0}$ self exchange and the solvent polarity parameter $E_T(30)$. While the solvent activation free energies, ΔG^*_{os}, extracted from the latter procedure are smaller than obtained from the former theoretical model, both analyses conclude that the electrochemical-exchange kinetics of all three hydrazine couples are markedly dependent upon the overdamped solvent dynamics. In contrast, the kinetics of $1^{+/0}$ self exchange are apparently insensitive to the solvent dynamics, the solvent-dependent rates reflecting chiefly variations in ΔG^*_{os}. These behavioral differences, along with the considerably more facile kinetics of electrochemical versus self exchange of $1^{+/0}$, are compared with the predictions of a theoretical model of coupled reactant vibrational-solvent dynamical activation by Sumi, Nadler, and Marcus (ref. 3) modified to account for nuclear tunneling and solvent inertia (ref. 17). The greater role of solvent dynamics, as well as the remarkably facile nature of the electrochemical exchange in comparison with the corresponding self-exchange reactions, can be rationalized on the basis of this theoretical treatment, although the observed degree of solvent-dynamical control is larger than predicted.

OFFICE OF NAVAL RESEARCH

Contract No. N00014-91-J-1409

Technical Report No. 132

Solvent Dynamical Effects in Electron Transfer: Electrochemical-Exchange Kinetics of Sesquibicyclic Hydrazines as a Probe of Coupled Vibrational Activation

by

Donald K. Phelps, Michael T. Ramm, Yichun Wang, Stephen F. Nelsen,

and Michael J. Weaver

Prepared for Publication

in

Journal of Physical Chemistry

Department of Chemistry

Purdue University

West Lafayette, Indiana 47907-1393

October 1992

ABSTRACT

Rate constants for electrochemical exchange of three sesquibicyclic hydrazine-radical cation redox couples, $k^{\bullet}_{ex}$, obtained at mercury by means of phase-selective ac voltammetry, are reported in seven solvents - acetonitrile, acetone, nitromethane, N, N-dimethylformamide, dimethylsulfoxide, benzonitrile and methanol. The hydrazine couples - denoted here $1^{+/0}$, $2^{+/0}$, and $3^{+/0}$ - feature variations in the bridgehead alkyl groups; they each exhibit substantial high-frequency vibrational barriers (4.5-5 kcal mol^{-1}) to electrochemical exchange. These systems therefore provide an interesting opportunity for the assessment of the manner and extent in which overdamped solvent relaxation may limit the electron-transfer dynamics under such circumstances. As in previous studies (ref. 2), scrutiny of the solvent-dependent rate constants enable at least semiquantitative estimates of the degree to which the kinetics are controlled by solvent dynamics as well as activation energetics. In addition to the usual dielectric-continuum treatment, estimates of the latter outer-shell component required for the solvent-dynamical analysis were acquired from an observed correlation between rates of $1^{+/0}$ self exchange and the solvent polarity parameter $E_T(30)$. While the solvent activation free energies, ΔG^{*}_{os}, extracted from the latter procedure are smaller than obtained from the former theoretical model, both analyses conclude that the electrochemical-exchange kinetics of all three hydrazine couples are markedly dependent upon the overdamped solvent dynamics. In contrast, the kinetics of $1^{+/0}$ self exchange are apparently insensitive to the solvent dynamics, the solvent-dependent rates reflecting chiefly variations in ΔG^{*}_{os}. These behavioral differences, along with the considerably more facile kinetics of electrochemical versus self exchange of $1^{+/0}$, are compared with the predictions of a theoretical model of coupled reactant vibrational-solvent dynamical activation by Sumi, Nadler, and Marcus (ref. 3) modified to account for nuclear tunneling and solvent inertia (ref. 17). The greater role of solvent dynamics, as well as the remarkably facile nature of the electrochemical exchange in comparison with the corresponding self-exchange reactions, can be rationalized on the basis of this theoretical treatment, although the observed degree of solvent-dynamical control is larger than predicted.

Unraveling the manner in which the kinetics of electron-transfer (ET) processes depend upon the solvent medium has attracted considerable attention over the last several years. Recent interest has focussed in particular on the likely influence of the solvent dynamical properties upon the ET barrier-crossing frequency.[1,2] While the qualitative presence of such overdamped dynamics on ET kinetics has been established in a number of cases, primarily from analyses of solvent-dependent rate data, a number of significant questions remain.[2] Not the least of these issues is the nature of the reaction dynamics for systems featuring activation barriers associated with inner-shell (reactant vibrational) distortions as well as solvent reorganization. This circumstance is indeed encountered in the large majority of experimental ET reactions. While conventional transition-state theory (TST) predicts that the faster inner-shell motions usually dominate the barrier-crossing dynamics, a distinctly different situation is anticipated in the presence of solvent friction, i.e., when the solvent dynamics are overdamped, in that the latter may well limit the barrier-crossing frequency.[2b]

An interesting theoretical treatment of this situation, having numerical predictive capability, has been described by Sumi, Nadler, and Marcus (referred to below as "SNM" theory).[3] Nevertheless, there is a surprising scarcity of experimental studies addressing this issue.[4-6] This situation is due in part to the paucity of outer-sphere ET reactions having well-defined (and preferably variable) inner-shell barriers alongside the other requirements for quantitatively viable solvent-dependent analyses. Of the various possibilities, nitrogen-centered molecule-radical redox couples constitute some attractive candidates since alterations in the structure of the N-substituents can yield large and variable inner shell barriers.[7]

The Wisconsin group has evaluated self-exchange rate constants for

sesquibicyclic hydrazine neutral–radical cation couples in various solvents by means of proton NMR line broadening.[8,9] These hydrazines exhibit much slower self–exchange rates than most organic redox couples, in the range 6.8×10^2 to 6.6×10^4 M^{-1} S^{-1} (vide infra). The small rates reflect in part the presence of sizable inner–shell barriers associated with distortions in the hydrazine core. A complication with such homogeneous ET reactions for the present purposes, however, is that the donor–acceptor orbital overlap within the ET transition state may often be insufficient to yield adiabatic reaction pathways, especially for organic reactions featuring high inner–shell frequencies. In that event, the barrier–crossing frequency will be determined at least partly by the electronic coupling rather than by nuclear reaction dynamics, thereby obscuring the assessment of the latter factor. There are reasons, however, to anticipate that the corresponding electrochemical–exchange reactions will proceed via distinctly more adiabatic pathways, thereby enabling the interplay between solvent–dependent dynamics and reactant vibrational activation to be explored with less possible hindrance from competing nonadiabatic effects. Besides the greater electronic coupling expected at metal surfaces on theoretical grounds,[10] several types of exchange reactions, including metallocenes[11,12] and p–phenylenediamines,[5,13] have been deduced experimentally to follow decidedly more adiabatic pathways in electrochemical than in homogeneous–phase environments.

We report here rate constants for molecule–radical cation electrochemical exchange, k_{ex}^{s}, of three sesquibicyclic hydrazines, 222/u222, 221/u222, and 221/222, (abbreviated here as 1, 2, and 3, respectively) having the structures shown in Fig. 1 below.

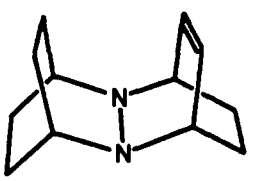

1

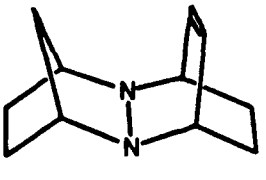

2

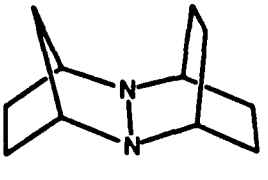

3

Electrochemical rate data were obtained by means of ac polarography at a dropping mercury electrode in seven solvents - acetonitrile, acetone, nitromethane, dimethylformamide, dimethylsulfoxide, benzonitrile, and methanol. As before,[4,11,12] these solvents were chosen since they provide polar media having a range of overdamped dynamics, as prescribed most simply by the longitudinal relaxation time, τ_L, thereby enabling the effect of varying the solvent friction upon the ET kinetics to be assessed. The first six solvents exhibit Debye (or near-Debye) dielectric behavior, hence displaying only a single major relaxation time. Inclusion of the last solvent, methanol, is prompted by its "non-Debye" nature: marked rate accelerations are apparent for several ET reactions in methanol and other primary alcohols as a result of faster solvent relaxation component(s) than τ_L.[2,11a,14-16] The solvent-dependent electrochemical rate behavior observed here is compared with corresponding data reported earlier[8a] for $1^{+/0}$ self exchange, and with numerical predictions obtained from a modified version of the SNM model described recently.[17] Overall, the present findings indicate the likely importance of overdamped solvent relaxation in limiting the adiabatic barrier-crossing frequency even in the face of substantial vibrational activation.

EXPERIMENTAL SECTION

The electrochemical rate constants, k°_{ex} (cm s^{-1}), were obtained by means of phase-selective ac voltammetry at a dropping mercury electrode, essentially as described in ref. 11a. This utilized a EG&G PAR 173/179 potentiostat with positive-feedback resistance compensation, a PAR 175 potential programmer, a PAR 5204 lock-in amplifier, and a Hewlett Packard 3314 function generator. The required reactant diffusion coefficients, D, were evaluated from the dc polarographic limiting currents. The solute concentration was typically ca 1 mM,

and the solvent was deaerated with argon. Purification of acetonitrile (Burdick and Jackson), acetone, methanol (Fisher), nitromethane (Kodak), and benzonitrile (Fluka) followed standard procedures;[18] N,N-dimethylformamide (DMF), and dimethylsulfoxide (DMSO) (Burdick and Jackson) were used without further purification. The supporting electrolyte, tetraethylammonium perchlorate (G.F. Smith), was recrystallized twice from hot ethanol. The sesquibicyclic hydrazines were synthesized as described previously.[8,19]

All electrode potentials were measured versus an aqueous saturated calomel electrode (SCE), and all electrochemical kinetic measurements were made at room temperature, 23±1°C.

RESULTS AND DISCUSSION

A summary of the rate constants for electrochemical exchange, $k^{\bullet}_{ex}$, determined here for the three hydrazine redox couples at mercury in seven solvents, each containing 0.1 M tetraethylammonium perchlorate (TEAP), is given in Table I. For convenience, this table also contains other parameters extracted from the polarographic data, specifically the formal potentials, E_f, for each redox couple/solvent combination, and diffusion coefficients, D, for the 222/u222 reactant. (The latter values for the other two reactants examined here, as might be expected, typically differ by less than 10–20% in a given solvent.) Most of the $k^{\bullet}_{ex}$ values fall in a range, ca 0.1–2 cm s^{-1}, which is amenable to reliable determination by the present ac impedance technique.[11a] The $k^{\bullet}_{ex}$ values were virtually unaffected (within ca 20%) upon increasing the TEAP concentration from 0.1 to 0.3 M. Values of the inverse longitudinal relaxation time, τ_L^{-1}, for each solvent are also listed in Table I.

For comparison, Table II lists rate constants for homogeneous self exchange of $1^{+/0}$, k^{h}_{ex}, in seven solvents, extracted from NMR line-broadening measurements

as reported in ref. 8, along with the corresponding τ_L^{-1} values. Six of these media, including four Debye solvents, are common to those in Table I. A summary of the electrochemical rate constants in acetonitrile for the three redox couples examined here in comparison with the available corresponding values for homogeneous self exchange is given in Table III.

Inner-Shell Activation Energies

Crystallographic data show that the oxidation of neutral hydrazines results in a large geometry change.[20] The lone-pair electron removed from a hydrazine is significantly antibonding, and the resulting radical cation contains a N–N 3e–π bond; these factors yield substantially different equilibrium geometries of the radical cation compared with the neutral parent.[21] This geometry change is largely responsible for the inner-shell activation barrier. A semiempirical MO calculation using the AM1 Hamiltonian[22] was used to calculate inner-shell reorganization energies for the three sesquibicyclic hydrazines shown in Fig. 1. A complete description of the method used to calculate these energies has been given elsewhere.[7] AM1 calculations have been shown to provide good estimates of the difference between vertical and adiabatic ionization potentials for hydrazines as measured by using high-pressure mass spectrometry.[23] It has been pointed out that the difference is approximately half of the inner-shell activation enthalpy.[7] (The other half is not presently experimentally measurable). Listed in Table III are the estimates of the inner-shell activation enthalpy for homogeneous self exchange of the three hydrazine couples, $\Delta H^*_{is,h}$, extracted from the semiempirical MO calculations. The corresponding activation enthalpies for electrochemical exchange, $\Delta H^*_{is,e}$, are necessarily one half of these values.[24]

The inner-shell barrier is strictly associated with a number of individual molecular motions, having a range of vibrational frequencies. An effective "net"

frequency as required for the present dynamical analysis may be extracted from a weighted average obtained from the usual formula[25] $\nu_q = (\sum_{j=1}^{n} \nu_j^2\lambda_j/\lambda)^{\frac{1}{2}}$, where λ_j is the reorganization energy component associated with each vibrational mode of frequency ν_j, and λ is the total reorganization energy. Using these parameters, extracted from the AM1 calculations, yielded values of ν_q close to 1500 (±50) cm^{-1} for all three hydrazine couples considered here. (Somewhat smaller estimates, ca 1000 cm^{-1}, are obtained from an alternate analysis;[26] these numerical differences, however, are not critical for the present purposes.)

Solvent-Dependent Rate Analyses

As noted above, of central interest here is the assessment of the degree to which the adiabatic barrier-crossing frequency is limited by overdamped solvent dynamics as compared with reactant vibrations. In order to utilize the present electron-exchange rate data for this purpose, as is usually the case it is necessary to disentangle the separate effects arising from the solvent dependencies of the nuclear dynamics and activation energetics.[2] One can express the rate constant for either electrochemical or homogeneous exchange reactions as[25,27]

$$k_{ex} = K_p \kappa_{el}\nu_n \exp\,[-(\Delta G^*_{os} + \Delta G^*_{is})/RT] \qquad (1)$$

Here K_p is the equilibrium constant (statistical probability) of forming the precursor state from the separated reactants, κ_{el} is the electronic transmission coefficient, ν_n is the nuclear frequency factor, and ΔG^*_{os} and ΔG^*_{is} are the outer-shell (i.e. solvent) and inner-shell (i.e. reactant vibrational) contributions, respectively, to the intrinsic free energy of activation.

Several distinct tactics have been utilized in the recent literature to correct the solvent-dependent rates for variations in ΔG^*_{os}, so to yield the required solvent-sensitivity of the reaction dynamics as described by $\kappa_{el}\nu_n$.[2]

Undoubtedly the most reliable procedure, especially for homogeneous self-exchange reactions, involves utilizing experimental estimates of ΔG^*_{os} extracted from optical ET energies measured for analogous binuclear redox systems.[28] While this procedure has proved invaluable for the analysis of metallocene self-exchanges,[2,12] no such optical data are as yet available for the sesquibicyclic hydrazines of concern here. Most commonly, the solvent-dependent ΔG^*_{os} values for both electrochemical and homogeneous-phase processes have been estimated by means of dielectric-continuum theory. While roughly applicable to near-spherical reactants such as the metallocenes, the reliability of this approach is in greater doubt for the hydrazines and other non-spherical systems. Indeed, an analysis for the self exchange of $1^{+/0}$ by the Wisconsin group shows that a significantly better correlation of the solvent-dependent kinetics are obtained with the Kosower Z parameter than with the "Pekar factor" used in the dielectric-continuum model.[8] As outlined below, the former suggests an alternative means of estimating the required solvent-dependent ΔG^*_{os} values.

Presuming for the moment that the solvent dependence of ΔG^*_{os} can be described approximately by the usual dielectric-continuum model, then we can rewrite Eq(1) as[2b,4b]

$$\log k_{ex} = \log \kappa_{el}\nu_n + \log K_p - \Delta G^*_{is}/2.3RT - C(\epsilon_{op}^{-1} - \epsilon_s^{-1}) \qquad (2)$$

where the components of the "Pekar factor" $(\epsilon_{op}^{-1} - \epsilon_s^{-1})$, ϵ_{op} and ϵ_s are the optical and static (i.e. zero-frequency) solvent dielectric constants, respectively. The "geometric factor" C in Eq(2) is usually estimated for electrochemical and homogeneous-phase reactions by the formulas[29]

$$C_e = (e^2/8)(r^{-1} - R_e^{-1}) \qquad (3a)$$

$$C_h = (e^2/4)(r^{-1} - R_h^{-1}) \qquad (3b)$$

where e is the electronic charge, r is the (presumed spherical) reactant radius, R_e is the reactant-metal image distance (i.e. twice the reactant-surface distance), and R_h is the homogeneous-phase coreactant separation, both within the appropriate precursor state. This separation of the dielectric-continuum energy barrier [last term in Eq(2)] into the geometric and Pekar factors is desirable given the likely uncertainties in the applicability of Eqs(3a) and (3b) for estimating the former. Thus the latter relations contain assumptions concerning reactant sphericity and electrode imaging effects that are unlikely to be quantitatively valid, especially for the present systems.[2,28,30] Fortunately, as noted below these uncertainties in the scaling term C do not necessarily invalidate the usefulness of the Pekar function contained in Eq(2).

An important limiting case is where the overall reaction dynamics (and hence $\kappa_{el}\nu_n$) are largely solvent-independent, as anticipated when electron tunneling and/or reactant vibrations dominate the barrier-crossing frequency.[2] Equation (2) then predicts that log k_{ex} should decrease approximately linearly with increasing $(\epsilon_{op}^{-1} - \epsilon_s^{-1})$. (This solvent-dependent analysis is referred to as "Method I" in ref. 2b.) Such behavior has been observed in several cases (eg. ref. 4b), and indeed is followed (albeit roughly) by the kinetics of $1^{+/0}$ self exchange.[8] For the present purposes, it is instructive to utilize relations such as Eq(2) to analyze the solvent-dependent kinetics of electrochemical exchange and homogeneous self exchange on an interchangeable basis. This can be achieved in part by transforming the measured k_{ex} values into "equivalent unimolecular" rate constants, (k_{ex}/K_p) (s^{-1}),[4b] with the precursor equilibrium constants for the electrochemical and homogeneous-phase reactions being estimated by the simple formulas[25,27]

$$K_p^o = \delta r_e \qquad (4a)$$

and

$$K_p^h = 4\pi N R_h^2 \, \delta r_h \qquad (4b)$$

Here N is Avogadro's number and δr_e and δr_h are the effective "reaction-zone thicknesses" describing the range of precursor geometries (involving close approach to the electrode and homogeneous coreactant, respectively) that provide the predominant contributions to the measured rates. For simplicity, both δr_e and δr_h can be taken as approximately 1Å, as is done here.[4b] The appropriate value of R_h is in greater doubt since the hydrazine reactants are clearly nonspherical. This value is taken here as 7Å, equal to twice the radius (3.5Å) of a sphere having the same volume as a cuboid (7.2 x 5.2 x 4.7Å) which will enclose the neutral hydrazine 1.[8,31] These values yield $K_p^h \simeq 0.2\underline{M}^{-1}$ from Eq(4b).

A plot of log (k_{ex}/K_p) versus $(\epsilon_{op}^{-1} - \epsilon_s^{-1})$, encompassing the electrochemical-exchange and homogeneous self exchange kinetics for $1^{+/o}$ (filled and open circles, respectively) is shown in Fig. 2. The rate data are taken from Tables I and II, using a common solvent numbering scheme as given in the tables. (The solvents in the latter were chosen so to optimize the degree of overlap with the present electrochemical data.) The straight line shown has an arbitrary y-displacement, but with a (negative) slope, C [Eq(2)], equal to that expected from Eqs(3a) and (3b) with r = 3.5Å, $R_h = 2r$, and $R_e^{-1} = 0$. (The condition $R_e^{-1} \to 0$ is tantamount to neglecting stabilizing reactant-imaging interactions for outer-sphere electrochemical reactions: its more general validity is supported by a more recent theoretical treatment.[30])

Both the electrochemical and homogeneous-phase rate data in Fig. 2 show significant scatter. A notable difference, however, is that the former (but not the latter) exhibit a *positive* log $k_{ex} - (\epsilon_{op}^{-1} - \epsilon_s^{-1})$ dependence, i.e., in *qualitative* disagreement with Eq(2) if $\kappa_{el}\nu_n$ is indeed solvent independent. As

noted elsewhere,[2b,4a,11a] such behavior for the present set of polar solvents signals a role of overdamped solvent relaxation in the overall reaction dynamics. This is because τ_L^{-1} tends to correlate roughly with $(\epsilon_{op}^{-1} - \epsilon_s^{-1})$ in polar media, so that the rate diminutions caused by higher activation barriers in more polar solvents [i.e. for larger $(\epsilon_{op}^{-1} - \epsilon_s^{-1})$] can be more than offset by the faster nuclear reaction dynamics (i.e. greater τ_L^{-1}) anticipated under these conditions.[2b]

An alternative graphical analysis, which can be instructive under these circumstances, entails correcting the rate constants for the anticipated solvent dependence of the activation barrier and examining how the observed "preexponential factor" $\kappa_{el}\nu_n(obs)$ thus evaluated depends on the solvent dynamics as prescribed most simply by τ_L^{-1}.[2b,4,32] This analysis (labelled "Method II" in ref. 2b) is usefully undertaken by reexpressing Eq(1) in the form

$$\log \kappa_{el}\nu_n(obs) = \log (k_{ex}/K_p) + (\Delta G_{os}^* + \Delta G_{is}^*)/2.3RT \qquad (5)$$

Given that ΔG_{is}^* will be essentially solvent independent, a plot of [log (k_{ex}/K_p) + $\Delta G_{os}^*/2.3RT$] versus log τ_L^{-1} can constitute a useful assessment of the role of solvent dynamics in the measured kinetics, provided that the solvent dependence of ΔG_{os}^* can be estimated satisfactorily.

Figure 3 displays a plot of this type for the same solvent-dependent rate data for $1^{+/o}$ as in Fig. 2. (The left- and right-hand y-axes refer to the electrochemical and homogeneous-phase rate data, respectively.) In addition to the electrochemical and homogeneous self exchange of $1^{+/0}$ (filled, open circles), data are also included for the electrochemical exchange of $2^{+/0}$ and $3^{+/0}$ (filled squares and triangles, respectively). The solvent-dependent ΔG_{os}^* values were estimated from the dielectric-continuum formula

$$\Delta G^{*}_{os} = C(\epsilon_{op}^{-1} - \epsilon_{s}^{-1}) \qquad (6)$$

with C given by Eqs(3a) or (3b), as appropriate, assuming that r = 3.5Å, R_h = 2r, and R_e^{-1} = 0, as above. The ΔG^{*}_{os} estimates obtained in this fashion, which are numerically equal for the electrochemical and homogeneous-phase processes in a given solvent, are listed in the left-hand column in Table IV. Inspection of Fig. 3 reveals several significant features. Not surprisingly given the form of Fig. 2 discussed above, the electrochemical exchange reaction displays a greater dependence of log $\kappa_{el}\nu_n$(obs) to log τ_L^{-1} than shown by the self-exchange process. Varying the magnitude of the "geometric factor" and hence the ΔG^{*}_{os} estimates, even by substantial factors (ca 30–40%), yielded relatively little change in the functional form of Fig. 3, indicating that the inevitable uncertainties in this "scaling term" do not significantly affect this conclusion. The analysis therefore infers that solvent dynamics play a greater role in the kinetics of the electrochemical process. Such behavior probably reflects the presence of a more adiabatic pathway, and/or a smaller contribution from vibrational dynamics, in the electrochemical reaction environment. These factors are considered further below.

As already mentioned, besides the uncertainties in the "scaling term" C, even the *functional form* of ΔG^{*}_{os} as prescribed by the Pekar factor in the dielectric-continuum model may be seriously in error for the present organic radical reactions. An alternative analysis is prompted by the observation in ref. 8 that log k^{h}_{ex} for $1^{+/0}$ self exchange in nine solvents, including three alcohols, correlates linearly with the Kosower Z or the closely related $E_T(30)$ solvent parameter. Interestingly, the correlation is markedly better than that observed between log k^{h}_{ex} and $(\epsilon_{op}^{-1} - \epsilon_{s}^{-1})$ (Fig. 2, open circles).[8] A reasonable (albeit not unique) interpretation is that the self-exchange dynamics of the $1^{+/0}$

are approximately solvent-independent, and the outer-shell (solvent) barrier scales more closely with Z or E_T (30) than with $(\epsilon_{op}^{-1} - \epsilon_s^{-1})$. Although this approach is necessarily semi-empirical,[2b] there is extensive evidence that the $E_T(30)$ and related solvent polarity scales can describe the solvent-dependent kinetics (and hence presumably the activation energetics) of a wide range of organic reactions in polar media.[33] This interpretation suggests a straightforward means by which "experimental" estimates of ΔG_{os}^* can be obtained; since the barrier is anticipated to disappear in the limit where $E_T(30) \approx 30$, one can write [cf Eq(2)].

$$\Delta G_{os}^* = [\log k_{ex}^h(30) - \log k_{ex}^h(E_T)] \; / \; 2.3\ RT \qquad (7)$$

where the second term in brackets refers to the rate constant for $1^{+/0}$ self exchange in a given solvent, and the first term is obtained by extrapolating the $\log k_{ex}^h - E_T(30)$ plot to $E_T(30) = 30$.

The ΔG_{os}^* values resulting from this analysis are listed in the far right-hand column of Table IV. Comparison with the dielectric-continuum ΔG_{os}^* estimates in the adjacent column shows that the former are markedly (ca twofold) smaller, even though a rough proportionality is preserved between the two set of values, reflecting the approximate correlation found between $E_T(30)$ and $(\epsilon_{op}^{-1} - \epsilon_s^{-1})$. Given that comparable values of ΔG_{os}^* are anticipated for hydrazine self exchange and electrochemical exchange in a given solvent (vide supra), there is justification for utilizing these $E_T(30)$ barrier estimates in place of the dielectric-continuum values in Eq(5). The plot resulting from this "alternative Method II" analysis is displayed for $1^{+/0}$, $2^{+/0}$, and $3^{+/0}$ electrochemical exchange in Fig. 4, in an analogous fashion to Fig. 3. (The corresponding data set for $1^{+/0}$ self exchange, shown in Fig. 3, is of course omitted from Fig. 4 since this yields necessarily a horizontal line.)

Not surprisingly given the disparate values of ΔG^*_{os} extracted from Eqs(6) and (7), the functional form of Fig. 4 (as well as the y-coordinate values) differs significantly from Fig. 3. Besides the additional scatter, the average slopes describing the three data sets in Fig. 4, ca 0.7–1.0, tend to be smaller than those, ca 1.0–1.2, in Fig. 3. This disparity arises from the smaller solvent dependence (as well as absolute values) of ΔG^*_{os} as extracted from the $E_T(30)$, compared with the dielectric-continuum, analysis. More significantly, however, the qualitative (or semi-quantitative) deduction that only the electrochemical processes exhibit a clearcut dependence on the dynamical solvent properties is seen to be unaffected by the choice of solvent-dependent barriers employed for the analysis.

Two other behavioral differences between the electrochemical and homogeneous-phase kinetics are readily evident from the above analyses. First, the former reaction yields unexpectedly facile kinetics in methanol (see points marked 7 in Figs. 3 and 4), whereas the latter process is relatively slow in methanol, as well as in other primary alcohols.[8] The former behavior is often observed for ET processes controlled by solvent dynamics, such as metallocenium-metallocene couples in both electrochemical and homogeneous-phase environments,[11a,12,15] and points to a dominant role of rapid relaxation components (i.e. those markedly faster than τ_L^{-1}) known to be present in primary alcohols in accelerating the barrier-crossing dynamics.[14,15] Second, the electrochemical data points in Fig. 3 are displaced upwards on the y-axis substantially (by 3–4 $\log_{10}$ units) compared with the corresponding entries for the homogeneous-phase process.

This latter difference is qualitatively unsurprising since the log $\kappa_{el}\nu_n$(obs) values estimated on the y-axis in Fig. 3 do not account for the presence of the inner-shell barrier. As already mentioned, the inner-shell

barrier for the self-exchange process, $\Delta G^*_{is,h}$, will necessarily be twice that for the corresponding electrochemical-exchange reaction, $\Delta G^*_{is,e}$.[23] Assuming that the inner-shell entropic barriers are negligible (as is likely the case), estimates of $\Delta G^*_{iv,e}$ and $\Delta G^*_{is,h}$ can be extracted directly from the $\Delta H^*_{is,h}$ estimates (obtained by AM1) listed in Table III. For $1^{+/o}$, then, $\Delta G^*_{is,h} = 2\Delta G^*_{is,e} = 9.0$ kcal mol^{-1}.

Comparison with Theoretical Predictions

At least at first sight, this estimated 4.5 kcal mol^{-1} difference between $\Delta G^*_{is,e}$ and $\Delta G^*_{is,h}$ can largely account for the 10^3-10^4 fold enhanced reactivities [i.e. larger (k_{ex}/K_p) values] observed for the electrochemical-exchange compared with the self-exchange reactions. It is desirable, however, to examine more closely the observed solvent-dependent kinetic behavior in Figs. 3 and 4 in comparison with contemporary theoretical predictions. As mentioned above, the Purdue group has recently undertaken numerical calculations of solvent-friction effects upon the barrier-crossing dynamics of reactions featuring vibrational barriers by means of a modified version of SNM theory.[17] Briefly, the SNM model envisages the reacting system progressing towards the barrier top predominantly by means of "solvent diffusion" (i.e. overdamped solvent motion), with the reaction being consummated in adiabatic fashion by motion along a separate vibrational coordinate.[3] An interesting qualitative feature of this treatment is that, unlike the TST picture, solvent relaxation can influence significantly the barrier-crossing dynamics even in the face of much more rapid vibrational motion by limiting the effective frequency at which the system approaches the barrier top. The chief modifications to the SNM model applied in ref. 17 involve allowing for nuclear tunneling along the high-frequency vibrational coordinate, and including barrier crossing by means of solvent inertial as well as reactant vibrational motion. The latter modification enables self-consistent numerical calculations to be undertaken in the absence as well as presence of a reactant

vibrational barrier.[17]

A set of logarithmic barrier-crossing frequencies relevant to Figs. 3 and 4, obtained for the present solvent set by using this modified SNM model, is plotted versus log τ_L^{-1} in Fig. 5. The y-axis of this plot, $\log(\Gamma_n\nu_n) - \Delta G^*_{is}/2.3RT$, where Γ_n is the nuclear-tunneling coefficient, is equivalent to the y-axis of the corresponding experimental plots in Figs. 3 and 4 since, as noted above, the latter is an estimate of the logarithmic barrier-crossing frequency, log $\kappa_{el}\nu_n$, minus $\Delta G^*_{is}/2.3RT$. (Note that the Γ_n term in Fig. 5 is necessary to account for rate accelerations brought about by nuclear tunneling through the vibrational barrier; the κ_{el} term is nonetheless absent in Fig. 5 since the SNM model presumes reaction adiabaticity.) The ΔG^*_{os} values were estimated as in Fig. 3. The reactant vibrational frequency was taken as 4.5×10^{13} s^{-1} (=1500 cm^{-1}, vide supra). Details of the calculational procedures are given in ref. 17. Three sets of solvent-(i.e. τ_L^{-1}-) dependent points for both the electrochemical (filled symbols) and self-exchange kinetics (open symbols) are included in Fig. 4. These refer to $\Delta G^*_{is,e}$ values of 2.5, 3.5, and 4.5 kcal mol^{-1} (filled triangles, squares, and circles, respectively); the corresponding $\Delta G^*_{is,h}$ values are twofold larger. The largest ΔG^*_{is} values employed in Fig. 5 ($\Delta G^*_{is,e}$ = 4.5 kcal mol^{-1}, $\Delta G^*_{is,h}$ = 9 kcal mol^{-1}, triangles) therefore correspond to the estimated inner-shell barriers for the $1^{+/o}$ couple (Table III).

In contrast to the experimental log $\kappa_{el}\nu_n$ - log τ_L^{-1} plots in Figs. 3 (and 4), these corresponding theoretical plots in Fig. 5 exhibit only a weak dependence of log $\Gamma_n\nu_n$ upon log τ_L^{-1}. Thus the log $\Gamma_n\nu_n$ - log τ_L^{-1} slopes for the electrochemical-exchange reaction (with $\Delta G^*_{is,e}$ = 4.5 kcal mol^{-1}), ca 0.1-0.2, are markedly smaller than the near-unit dependencies of log $\kappa_{el}\nu_n$ upon log τ_L^{-1} inferred from the experimental data in Fig. 3. As expected, diminishing $\Delta G^*_{is,e}$ has the effect of enhancing the predicted sensitivity of the rate to the solvent

dynamics; thus log $\Gamma_n\nu_n$ - log τ_L^{-1} slopes of 0.3–0.4 are obtained for $\Delta G^*_{is,e}$=2.5 kcal mol^{-1} (Fig. 5), still smaller than are observed experimentally. The predicted slopes are also seen to decrease towards larger $\log_{10}\tau_L^{-1}$ as a result of the increasingly limiting influence of solvent inertia;[17,34] this effect is not evident, however, in the experimental data. Similar conclusions are reached if the results of the alternative solvent–dependent analysis in Fig. 4 are compared with the theoretical SNM predictions. Thus while the average log $\kappa_{el}\nu_n$ - log τ_L^{-1} slopes extracted from Fig. 4 are somewhat (ca 20–30%) smaller than from Fig. 3, the corresponding ΔG^*_{os} estimates in the former case are about twofold smaller, so that ($\Delta G^*_{is}/\Delta G^*_{os}$) is twofold larger. Still smaller log $\Gamma_n\nu_n$ - log τ_L^{-1} slopes are predicted from the SNM model under these conditions (Fig. 5).

Nevertheless, some other aspects of the experimental results are mimicked at least semiquantitatively by the theoretical calculations. The homogeneous–phase reactivities (for $\Delta G^*_{is,h}$ = 9 kcal mol^{-1}) are predicted to be markedly (20–30 fold) smaller than for the corresponding electrochemical process, as discerned from the y–displacement in Fig. 5. The larger (10^2–10^3 fold) observed reactivity difference as discerned from Fig. 3 may reflect the presence of less adiabatic pathways for the self–exchange process (and possibly larger outer–shell barriers) than for the electrochemical reactions. In harmony with this assertion, the y–axis values for the self–exchange reaction in Fig. 3 (open circles) are substantially (10–50 fold) smaller than the corresponding calculated values (open triangles) in Fig. 5.

An interesting feature of the theoretical predictions concerns the dependence of the rate constants upon the magnitude of the inner–shell barrier. For this purpose, Fig. 6 displays a logarithmic plot of the equivalent unimolecular rate constant, log (k_{ex}/K_p), versus the ratio of inner– to outer–shell barriers, $\Delta G^*_{is}/\Delta G^*_{os}$, for a sequence of four log τ_L^{-1} values as labelled. As

in Fig. 5, the reactant vibrational frequency is taken as 4.5×10^{13} s^{-1}; ΔG^*_{os} is fixed at 4 kcal mol^{-1}. The set of solid and dashed traces were calculated with and without consideration of nuclear tunneling, respectively. Comparison between these calculated data sets shows the marked influence of nuclear tunneling in both enhancing the rate and accentuating the degree to which solvent relaxation still influences the reaction dynamics in the presence of the inner-shell barrier. The latter is evident from the substantially larger y-displacements seen for a given $(\Delta G^*_{is}/\Delta G^*_{os})$ value, especially for $(\Delta G^*_{is}/\Delta G^*_{os}) > 0.5$. (Further details are available in ref. 17.) Significantly, Fig. 6 shows that the inclusion of the inner-shell barrier *increases* the reaction rate, at least for $(\Delta G^*_{is}/\Delta G^*_{os}) \lesssim 0.5$. (The crosses marked on the y-axis denote the log (k_{ex}/K_p) values in the absence of the inner-shell barrier.) This effect is due to the marked accelerations in the barrier-crossing dynamics arising from the high-frequency reactant vibrations more than offsetting the progressively larger activation barrier present under these conditions. As ΔG^*_{is} is increased, however, the latter factor eventually dominates, yielding a maximum in the log (k_{ex}/K_p) - $(\Delta G^*_{is}/\Delta G^*_{os})$ dependence for a given r_L value (Fig. 6).

These considerations can also account for the remarkably facile electrochemical exchange kinetics observed for the present sesquibicyclic hydrazine couples. Thus the solvent-dependent k^o_{ex} values in Table I are comparable to those observed for numerous redox couples that are known to involve only small or negligible inner-shell barriers. For example, the present k^o_{ex} values are only ca 2.5 fold smaller than those observed for $Cp_2Co^{+/o}$ and other metallocene couples at mercury,[11a] even though the latter system has only a small $\Delta G^*_{is,o}$ value, ca 0.7 kcal mol^{-1}.[35] Provided that the outer-shell barriers for these systems are roughly similar (as expected) and that adiabatic pathways are followed, then the comparable k^o_{ex} values observed for the sesquibicyclic hydrazine and metallocene

redox couples infer that the rapid vibrational dynamics for the former systems act to offset almost entirely the rate-decelerating effect of the larger activation barriers.

Comparison between the kinetics of the corresponding homogeneous self-exchange reactions is also instructive in this regard. For example, the k_{ex}^{h} value for $Cp_2Co^{+/o}$ self exchange in acetonitrile, 4.5×10^7 M^{-1} s^{-1},[12] is markedly (4×10^3 fold) greater than for $1^{+/o}$ self exchange under the same conditions. Given that the hydrazine self-exchange process necessarily involves an inner-shell barrier that is twice that for electrochemical exchange, the sharply diminished reactivity of the former reaction in comparison with $Cp_2Co^{+/o}$ self exchange is probably due in part to a more dominant decelerating influence of the activation energetics. In addition, as noted above, the hydrazine self exchange may well proceed via weakly adiabatic or even nonadiabatic pathways, depressing further the reaction rate.

Finally, it is appropriate to comment on the observed rate differences between the three hydrazine couples in this context. While the order of k_{ex}^{e} values in a given solvent tends to be $1^{+/o} > 2^{+/o} \gtrsim 3^{+/o}$ (Table I), the rate differences tend to be fairly small (threefold or less). This insensitivity of the electrochemical rates to the hydrazine structure again probably reflects offsetting variations in the vibrational dynamics and energetics. Nevertheless, the AM1 calculations suggest that the inner-shell barriers for these redox couples do not differ greatly (Table III). Thus the 0.6 kcal mol^{-1} smaller $\Delta H_{is,h}^{\ddagger}$ value for the $1^{+/o}$ versus the $2^{+/o}$ couple corresponds to predicted k_{ex}^{h} and k_{ex}^{e} values for the former which are only ca 3 fold and 1.5 fold larger, respectively, than for the latter. (This estimate neglects differences in nuclear tunneling and other dynamical factors between the two systems.)

CONCLUDING REMARKS

While a truly quantitative analysis of the observed solvent-dependent kinetics is thwarted by the usual difficulties in separating reliably the dynamical and energetic contributions, the present results add significantly to the extant evidence[4-6] that solvent friction can exert a noticeable influence upon the barrier-crossing dynamics even in the presence of substantial (several kcal mol^{-1}) activation barriers arising from reactant vibrational rearrangements. The role of overdamped solvent dynamics is more clearly evident for electrochemical exchange, but not for the homogeneous-phase self-exchange processes. This difference probably reflects the presence of more adiabatic pathways as well as smaller inner-shell barriers for the former reaction type. It would clearly be desirable to obtain direct experimental information on the solvent-dependent activation barriers from optical ET energy measurements on symmetrical mixed-valence binuclear hydrazines. Substantial efforts along these lines are underway in the Wisconsin group..

On the basis of the present findings, the SNM model would appear to underestimate the importance of solvent dynamical effects to the adiabatic barrier-crossing frequency in the presence of substantial reactant vibrational activation. Nevertheless, the theoretical model describes in at least a qualitatively correct manner the remaining influence upon the reaction dynamics exerted by such slow overdamped solvent relaxation even in the presence of the considerable rate accelerations brought about in the presence of much more rapid vibrational motion. One limitation of the theoretical model is that it presumes the presence of a cusp-shaped barrier: substantial barrier-top roundedness is expected in practice given the degree of donor-acceptor electronic coupling necessary for control of the reaction dynamics by overdamped solvent relaxation (or other nuclear motion).[17] The development of theoretical dynamical treatments

which incorporate these and other features would certainly be worthwhile.

ACKNOWLEDGMENTS

This work is supported by grants from the Office of Naval Research (to M.J.W.) and the National Institutes of Health (Grant GM. 29547, to S.F.N.).

REFERENCES AND NOTES

1. (a) Barbara, P.F.; Jarzeba, W., Adv. Photochem., **1990**, 15, 1; (b) Maroncelli, M.; MacInnis, J.; Fleming, G.R., Science, **1989**, 243, 1674; (c) Bagchi, G., Ann. Rev. Phys. Chem., **1989**, 40, 115; (d) Fleming, G.R.; Wolynes, P.G., Physics Today, **1990**, 43 (May), 36

2. (a) Weaver, M.J.; McManis, G.E., Acc. Chem. Res., **1990**, 23, 294; (b) Weaver, M.J., Chem. Rev., **1992**, 92, 463

3. (a) Sumi, H.; Marcus, R.A., J. Chem. Phys., **1986**, 84, 4894; (b) Nadler, W.; Marcus, R.A., J. Chem. Phys., **1987**, 86, 3906; (c) also see: Marcus, R.A., Sumi, H., J. Electroanal. Chem., **1986**, 204, 59

4. (a) Nielson, R.M.; Weaver, M.J., J. Electroanal. Chem., **1989**, 260, 15; (b) Weaver, M.J.; Phelps, D.K.; Nielson, R.M.; Golovin, M.N.; McManis, G.E., J. Phys. Chem., **1990**, 94, 2949

5. Grampp, G.; Jaenicke, W., Ber. Bunsenges. Phys. Chem., **1991**, 95, 904

6. Su, S.-G.; Simon, J.D., J. Chem. Phys., **1988**, 89, 908

7. (a) Nelsen, S.F.; Blackstock, S.C.; Kim, Y., J. Am. Chem. Soc., **1987**, 109, 677; (b) Nelsen, S.F., "Advances in Electron-Transfer Chemistry", Vol. 3, Mariano, P.S., ed, JAI Press, Greenwich, CT, in press.

8. Nelsen, S.F.; Kim, Y.; Blackstock, S.C., J. Am. Chem. Soc., **1989**, 111, 2045

9. Nelsen, S.F.; Wang, Y.; Ramm, M.T.; Accola, M.A.; Pladziewicz, J.R., J. Phys. Chem., in press.

10. (a) Morgan, J.D.; Wolynes, P.G., J. Phys. Chem., **1987**, 91, 874; (b) Zusman, L.D., Chem. Phys., **1987**, 112, 53

11. (a) McManis, G.E.; Golovin, M.N.; Weaver, M.J., J. Phys. Chem., **1986**, 90, 6563; (b) Nielson, R.M.; Golovin, M.N.; McManis, G.E.; Weaver, M.J., J. Am. Chem. Soc., **1988**, 110, 1745

12. McManis, G.E.; Nielson, R.M.; Gochev, A.; Weaver, M.J., J. Am. Chem. Soc., **1989**, 111, 5533

13. Kapturkiewicz, A., Jaenicke, W., J. Phys. Soc. Far. Trans. I, **1987**, 83, 2727

14. McManis, G.E.; Weaver, M.J., J. Chem. Phys., **1989**, 90, 912

15. (a) Nielson, R.M.; McManis, G.E.; Weaver, M.J., J. Phys. Chem., **1989**, 93, 4703; (b) Weaver, M.J.; McManis, G.E.; Jarzeba, W.; Barbara, P.F., J. Phys. Chem., **1990**, 94, 1715

16. (a) Opallo, M.; Kapturkiewicz, A., Electrochim. Acta, **1985**, 30, 1301; (b) Opallo, M., J. Chem. Soc. Far. Trans. I, **1986**, 82, 339

17. Phelps, D.K.; Weaver, M.J., J. Phys. Chem., **1992**, 96, 7187

18. (a) Perrin, D.D.; Armarego, W.L.F.; Perrin, D.R., "Purification of Laboratory Chemicals", 2nd Edn., Pergamon, New York, 1980; (b) Riddick, J.A.; Bunger, W.B.; Sakano, T.K., "Organic Solvents-Physical Properties and Methods of Purification", 4th Edn., Wiley, New York, 1986.

19. (a) Nelsen, S.F.; Blackstock, S.C.; Frigo, T.B., J. Am. Chem. Soc., **1984**, 106, 3366; (b) Nelsen, S.F.; Blackstock, S.C.; Frigo, T.B., Tetrahedron, **1986**, 42, 1769

20. Nelsen, S.F.; Blackstock, S.C.; Haller, K.J., Tetrahedron, **1986**, 42, 6101

21. (a) Nelsen, S.F., in "Molecular Structures and Energetics," Liebman, J.F., Greenberg, A., Eds, VCH Publishers, Deerfield Beach, FL, 1986, Vol. 3, Chapter 1; (b) Nelsen, S.F., Acc. Chem. Res. **1981**, 14, 131

22. Dewar, M.J.S.; Zoebisch, E.G.; Healy, E.F.; Stewart, J.P., J. Am. Chem. Soc., **1985**, 107, 3902

23. (a) Nelsen, S.F., Rumack, D.T., Meot-Ner (Mautner), M., J. Am. Chem., Soc., **1988**, 110, 7945; (b) Nelsen, S.F., Rumack, D.T., Meot-Ner (Mautner), M., J. Am. Chem. Soc., **1987**, 109, 1373

24. The relationship $\Delta H^{*}_{is,s} = 0.5\ \Delta H^{*}_{is,h}$ (or the corresponding identity involving activation free energies) arises simply because only one reacting species is required to undergo activation in electrochemical exchange, as compared to a pair of reactants for homogeneous self exchange.

25. See for example: Sutin, N., Prog. Inorg. Chem., **1983**, 30, 441

26. Because AM1 calculations yield the result that differences in thermodynamics of oxidation for different sesquibicyclic hydrazines are linearly related to the average of the dihedral angles at N (α(av)), the Wisconsin group carried out a non-conventional estimation of ν_q in which the fractional change in α(av) towards the ET transition state instead of λ_j/λ was used to weigh ν_j^2 in the summation. This procedure produced estimates for ν_q of 1120 cm^{-1} for 1 and of 970 cm^{-1} for the standard compound related to 1.

27. Hupp, J.T.; Weaver, M.J., J. Electroanal. Chem., 1983, 152, 1

28. McManis, G.E., Gochev, A., Nielson, R.M., Weaver, M.J., J. Phys. Chem, 1989, 93, 7733

29. Marcus, R.A., J. Chem. Phys., 1965, 43, 679

30. (a) Dzhavakhidze, P.G.; Kornyshev, A.A.; Krishtalik, L.I., J. Electroanal. Chem., 1987, 228, 329; (b) Phelps, D.K.; Kornyshev, A.A.; Weaver, M.J., J. Phys. Chem., 1990, 94, 1454

31. The radii of spheres having the same volume as the optimized AM1 structures of 1-3 are slightly smaller: 3.33, 3.25, and 3.27Å, respectively. Essentially the same values are calculated for the neutral and radical cation forms. The procedure used sums the volumes of spheres having the Van der Waals radii of the atoms, centered at the positions calculated for the optimized structures, with the overlapping regions subtracted.

32. Neilson, R.M.; McManis, G.E.; Golovin, M.N.; Weaver, M.J., J. Phys. Chem., 1988, 92, 3441

33. For example, see: Reichardt, C., "Solvent Effects in Organic Chemistry", Verlag Chemie, New York, 1979.

34. McManis, G.E.; Gochev, A.; Weaver, M.J., Chem. Phys., 1991, 152, 107

35. See footnote 47 of ref. 12, recalling that[24] $\Delta G^*_{is,e} = 0.5\ \Delta G^*_{is,h}$

TABLE I Rate Constants for Electrochemical Exchange, k_{ex}, of Sesquibicyclic Hydrazine-Radical Cation Couples in Various Solvents, and Related Solvent-Dependent Parameters

No.	Solvent	τ_L^{-1}[a] 10^{12} s^{-1}	D[b] $10^{-5}cm^2$ s^{-1}	E_f, V vs SCE[c] $1^{+/0}$	$2^{+/0}$	$3^{+/0}$	k°_{ex}, cm s^{-1}[d] $1^{+/0}$	$2^{+/0}$	$3^{+/0}$
1	Acetonitrile	4	1.6	-0.26	0.04	-0.19	2.4	1.0	0.9
2	Acetone	3.5	1.6	-0.18	0.14	-0.05	0 6	1.2	0.4
3	Nitromethane	4.5	0.6	-0.33	-0.03	-0.24	0.75	0.7	0.5
4	Dimethyl-formamide	0.77	0.4	-0.14	0.14	-0.09	0.28	0.3	e
5	Dimethyl-sulfoxide	0.5	0.3	-0.18	0.10	-0.10	0.22	0.14	0.2
6	Benzonitrile	0.2	0.3	-0.25	)5	-0.17	0.4	0.30	0.15
7	Methanol	(0.135)	1.5	-0.16	.14	-0.06	3.9	1.6	~1.0

[a] Inverse longitudinal relaxation time for indicated solvent, from data compilation in Table I of ref. 12. (Methanol value given in parentheses since additional higher-frequency dispersive component is also evident.)

[b] Diffusion coefficient for hydrazine 1 in indicated solvent, obtained from dc polarographic limiting current. (Values for other hydrazines typically within ±10-20% in a given solvent.)

[c] Formal potential for stated +/o hydrazine redox couple in indicated solvent, obtained from ac polarography.

[d] Rate constant for electrochemical exchange for stated +/o hydrazine redox couple in indicated solvent containing 0.1 M TEAP, obtained from ac polarography. Values generally reproducible to ca ±10-20%.

[e] Reliable estimate of k°_{ex} for this system precluded by anomalously asymmetric ac polarograms (due probably to incipient reactant adsorption or related effects).

TABLE II Rate Constants for Self Exchange of $1^{+/o}$ in Selected Solvents (from ref. 8)

No.	Solvent	τ_L^{-1} [a] 10^{12} s^{-1}	k_{ex}^h [b] M^{-1} s^{-1}
1	Acetonitrile	4	$1.2_1 \times 10^4$
3	Nitromethane	4.5	$2.3_5 \times 10^4$
4	Dimethylformamide	0.77	$2.1_7 \times 10^4$
5	Dimethylsulfoxide	0.5	$1.0_4 \times 10^4$
7	Methanol	(0.135)	6.8×10^2
8	Ethanol	(0.033)	2.2×10^3
9	Pyridine	~1.0	$6.5_8 \times 10^4$

[a] Inverse longitudinal relaxation time for indicated solvent, from data compilation in Table I of ref. 12. (Values for methanol and ethanol given in parentheses to denote non-Debye behavior.)

[b] Rate constant for homogeneous self exchange of $1^{+/o}$ in solvent indicated, taken from ref. 8.

TABLE III Comparison between Electrochemical and Homogeneous Exchange of Sesquibicyclic Hydrazines in Acetonitrile with Calculated Reactant Reorganization Barrier.

Redox Couple	k_{ex}^{e} [a] cm s^{-1}	k_{ex}^{h} [b] M^{-1} s^{-1}	$\Delta H^{*}_{is,h}$ [c] kcal mol^{-1}
$1^{+/o}$	2.4	1.2×10^{4}	9.1
$2^{+/o}$	1.0	2.3×10^{3}	9.7
$3^{+/o}$	0.9		9.3

[a] Rate Constants for Electrochemical Exchange in Acetonitrile, from Table I

[b] Rate Constants for Homogeneous Self Exchange in Acetonitrile, from ref. 9

[c] Inner-shell activation enthalpy for self exchange, determined from AM1 semiempirical MO calculation (see ref. 7)

TABLE IV Estimated Outer-Shell Barriers, ΔG^{*}_{os}, for Sesquibicyclic Hydrazine Electrochemical Exchange used in Figures 3 and 4.

No.	Solvent	ΔG^{*}_{os}, kcal mol^{-1}	
		Eq(6)[a]	Eq(7)[b]
1	Acetonitrile	6.25	2.85
2	Acetone	5.85	2.2
3	Nitromethane	5.90	2.45
4	Dimethylformamide	5.5	2.5
5	Dimethylsulfoxide	5.2	2.95
6	Benzonitrile	4.55	2.05
7	Methanol	6.35	2.2

[a] Values estimated from dielectric-continuum model [Eqs(3b), (6)], with r=3.5Å, R_h=2r (see text).

[b] Values estimated from solvent-dependent analysis of rate constants for $1^{+/0}$ self exchange (taken from ref. 8) according to Eq(7) (see text).

FIGURE CAPTIONS

Figure 1

Molecular structures of the three sesquibicyclic hydrazines examined here.

Figure 2

Plot of logarithm of "unimolecular" rates constant for $1^{+/0}$ electrochemical exchange (filled circles) and self exchange (open circles) versus the solvent Pekar factor. Rate data (and solvent numbering scheme) from Tables I and II, with K_p^e and K_p^h extracted from Eqs(4a) and (4b), respectively. The straight line shown (having arbitrary y-displacement) has slope obtained from Eq (3a) or (3b) with r=3.5Å, r_h=2r, and R_e^{-1}=0 (see text).

Figure 3

Logarithmic plot of unimolecular rate constant, corrected for outer-shell barrier ΔG^*_{os}, for $1^{+/0}$, $2^{+/0}$, and $3^{+/0}$ electrochemical exchange (filled circles, squares, and triangles, respectively) and $1^{+/0}$ self-exchange (open circles) versus the inverse solvent longitudinal relaxation time. Values of ΔG^*_{os} (Table IV) estimated from Eqs(3) and (6), with r=3.5Å, R_h=2r, and R_e^{-1}=0 (see text). Rate data (and solvent numbering scheme) from Tables I and II. The solvent τ_L values were taken from compilations in refs. 11 and 12. The points for methanol (7) are given in parenthesis since this solvent exhibits marked non-Debye behavior.

Figure 4

As in Fig. 3 for electrochemical exchanges, but with ΔG^*_{os} values (Table IV) estimated from log k^h_{ex} - $E_T(30)$ correlation by using Eq(7).

Figure 5

Logarithmic plot of predicted barrier-crossing frequency (corrected for inner-shell barrier ΔG^*_{is}) as obtained from modified SNM model[17] versus inverse longitudinal relaxation time in selected solvents for various ΔG^*_{is} values, as follows: Filled triangles, circles, and squares; 2.5, 3.5 and 4.5 kcal mol^{-1}, respectively. Corresponding open symbols refer to ΔG^*_{is} values twofold larger (thereby mimicking barriers for self-exchange versus electrochemical exchange reactions). Solvent-dependent ΔG^*_{os} values estimated from Eq(6) (Table IV). The solvent τ_L values are taken from compilations in refs. 11 and 12; solvent

inertial limiting frequencies (also required for theoretical analysis) as in refs. 14 and 32. Solvents are from left to right: methanol, benzonitrile, DMSO, DMF, nitromethane, acetone, and acetonitrile. Reactant average vibrational frequency, ν_q, taken as $4.5 \times 10^{13} s^{-1}$ ($\approx$1500 cm^{-1}) (see text and ref. 17 for further details).

Figure 6

Plot of logarithm of unimolecular rate constant as predicted by modified SNM model[17] for various log (τ_L^{-1}, s^{-1}) values, as indicated, versus ratio of inner- to outer-shell activation barriers, with latter (ΔG^*_{os}) held fixed at 4 kcal mol^{-1}. Reactant vibrational frequency, ν_q, taken as $4.5 \times 10^{13} s^{-1}$, and solvent inertial frequency ($\omega_o/2\pi$) held fixed at "typical value,"[32] $1.8 \times 10^{12} s^{-1}$. The solid and dashed curves were calculated by including and omitting nuclear-tunneling effects, respectively, along the vibrational reaction coordinate (see ref. 17 for further details).

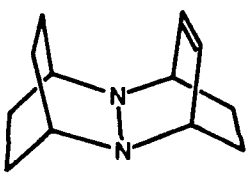

1

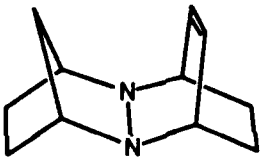

2

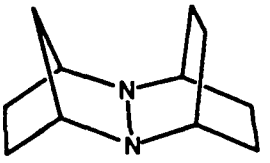

3

FIG 1

a:weav.ftr

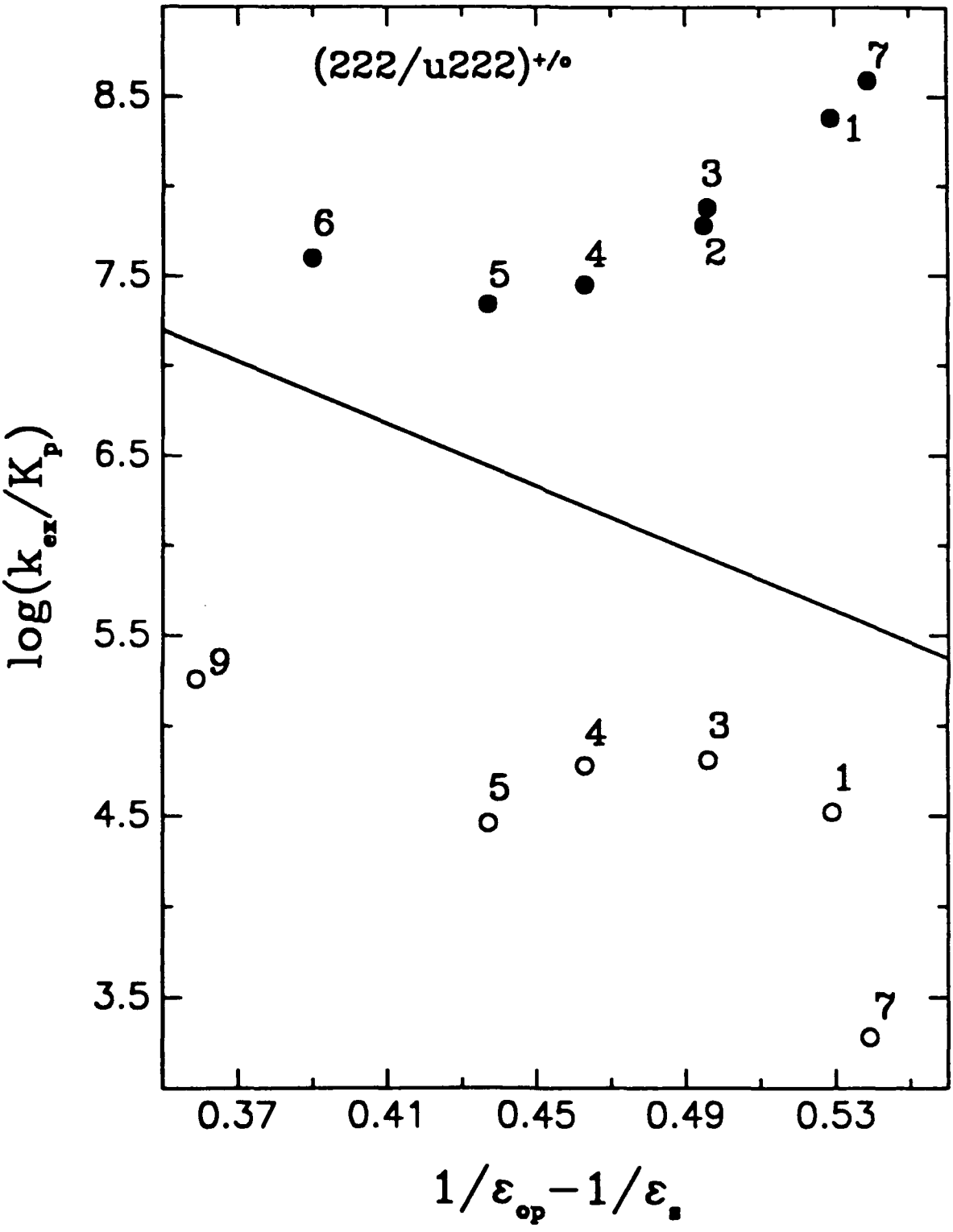
(222/u222)+/o
8.5
7.5
6.5
5.5
4.5
3.5
log(k_ex/K_p)
0.37
0.41
0.45
0.49
0.53
1/ε_op − 1/ε_s
7
1
3
2
6
5
4
9
4
3
5
1
7

FIG 2

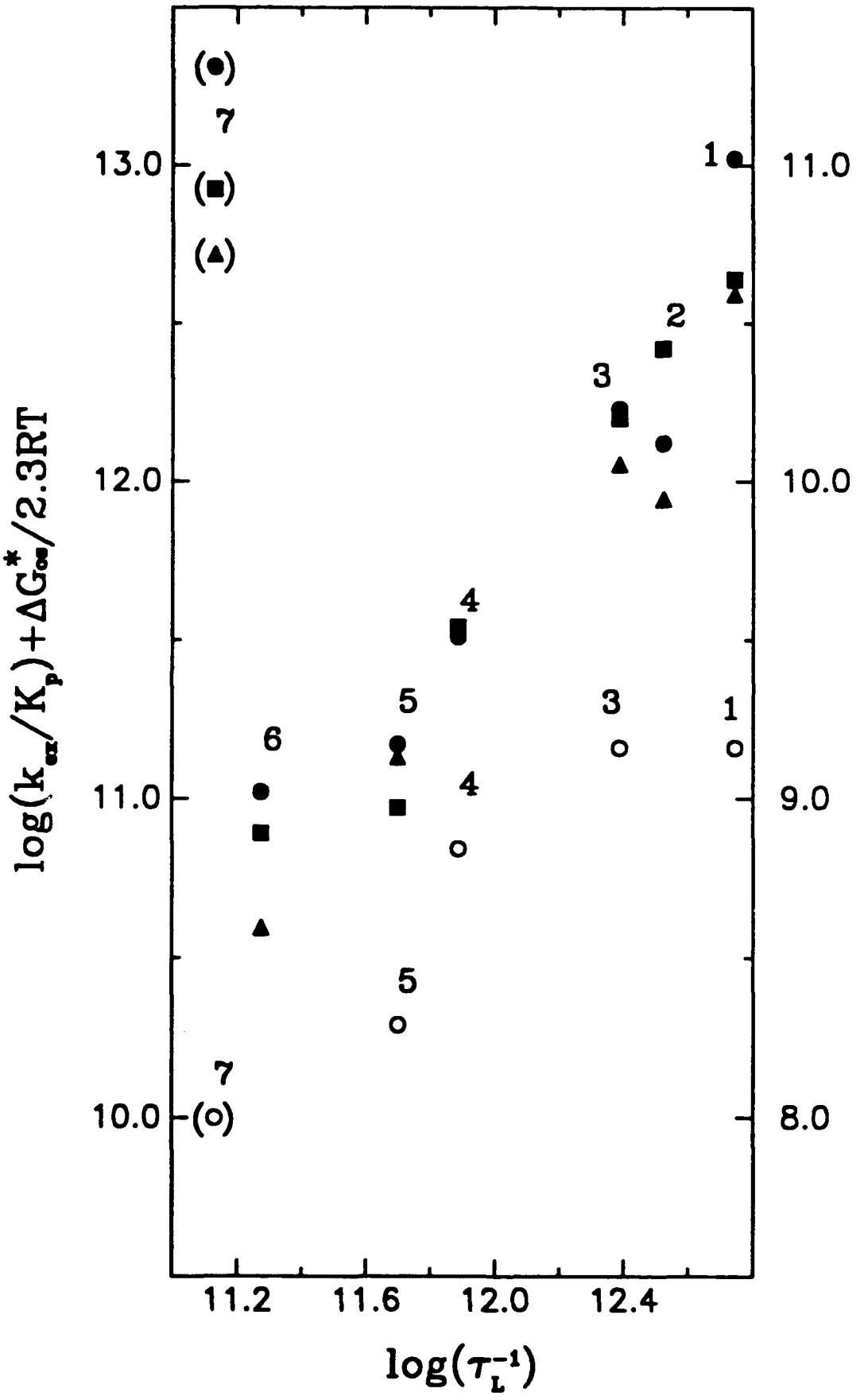
(●)
7
(■)
(▲)
13.0
12.0
11.0
10.0
1
2
3
4
5
6
7
(○)
11.0
10.0
9.0
8.0
11.2
11.6
12.0
12.4
log(k∞/Kp)+ΔG*∞/2.3RT
log(τL⁻¹)

FIG 3

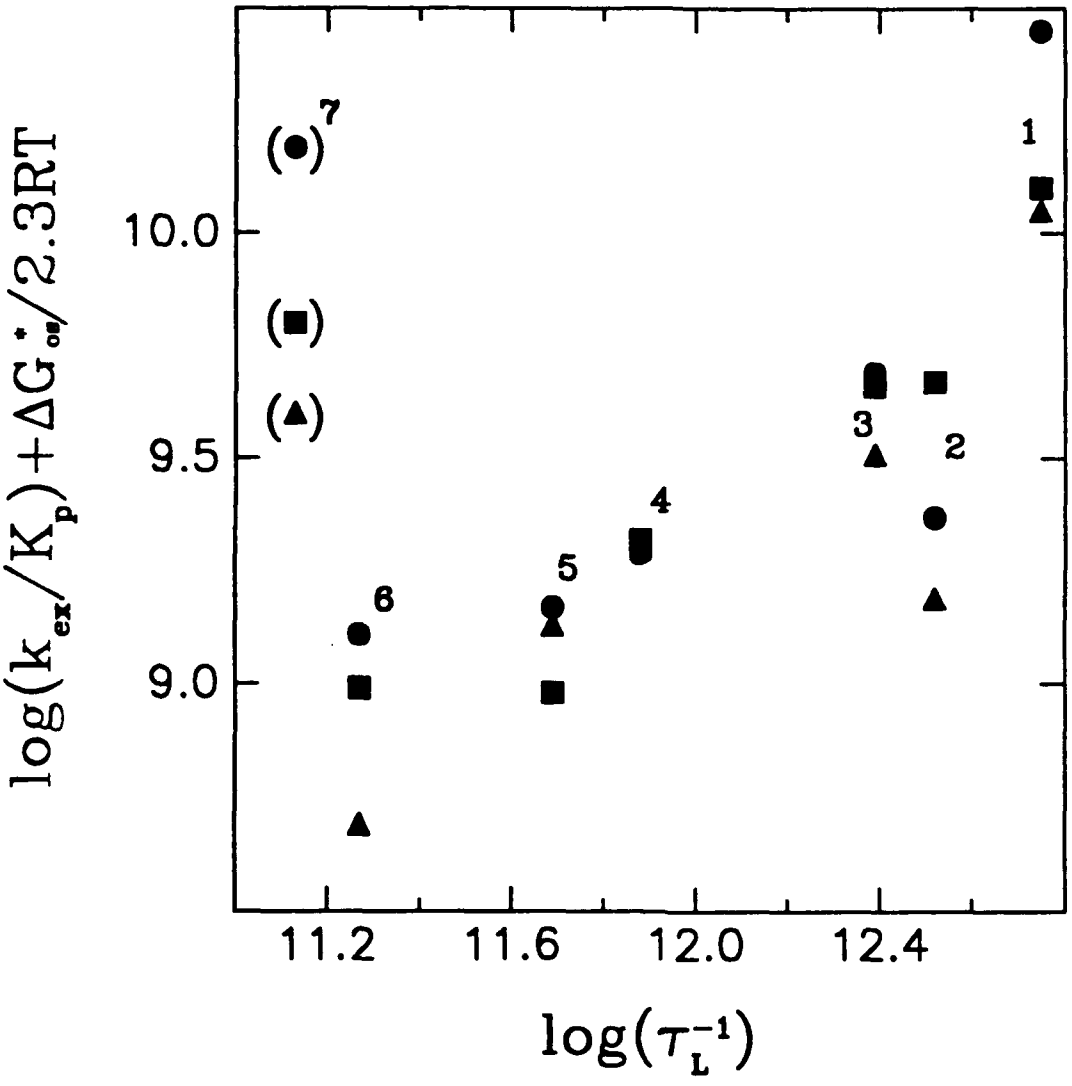

FIG 4

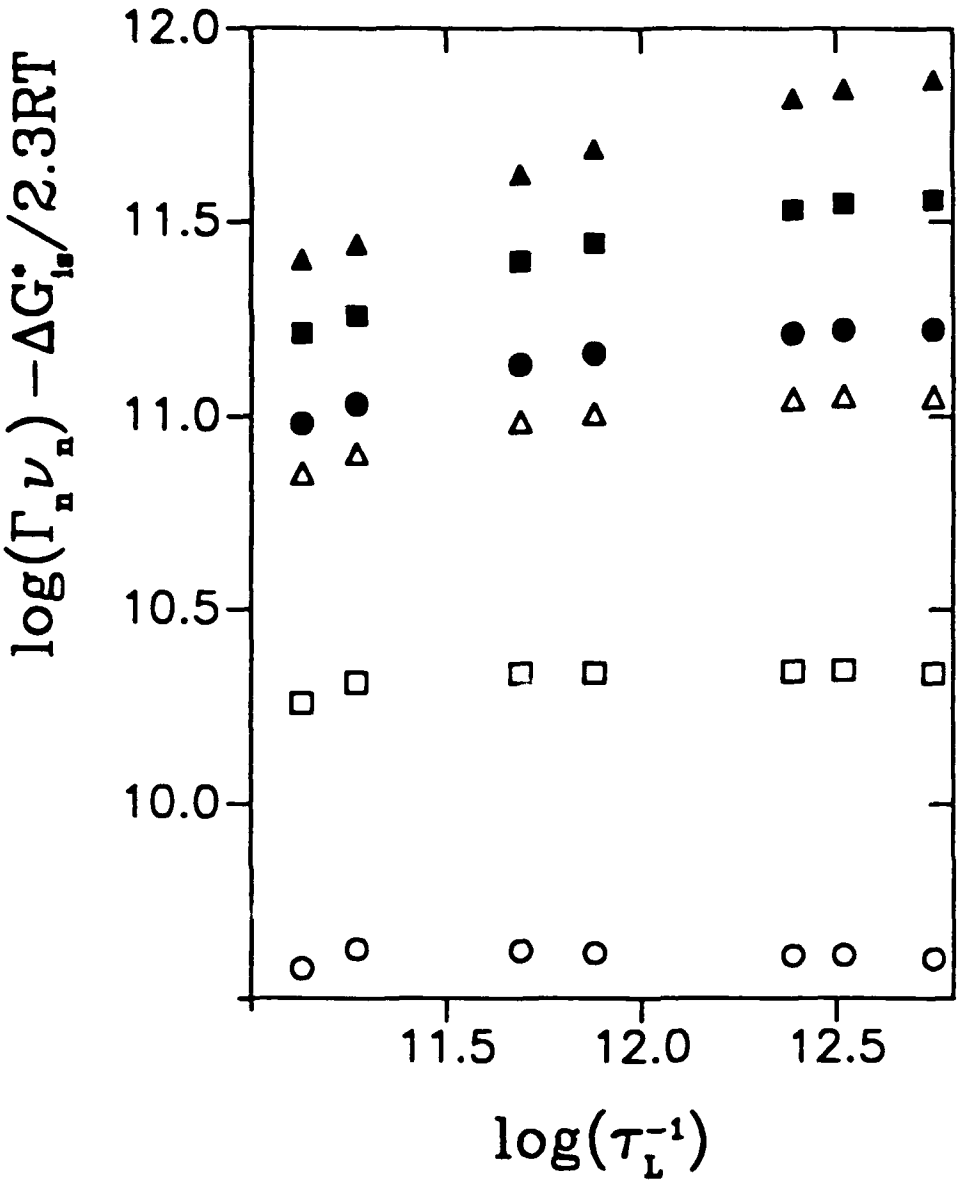
12.0
11.5
11.0
10.5
10.0
11.5
12.0
12.5
$\log(\Gamma_n \nu_n) - \Delta G^{\ddagger}_{1n}/2.3RT$
$\log(\tau_L^{-1})$

FIG 5

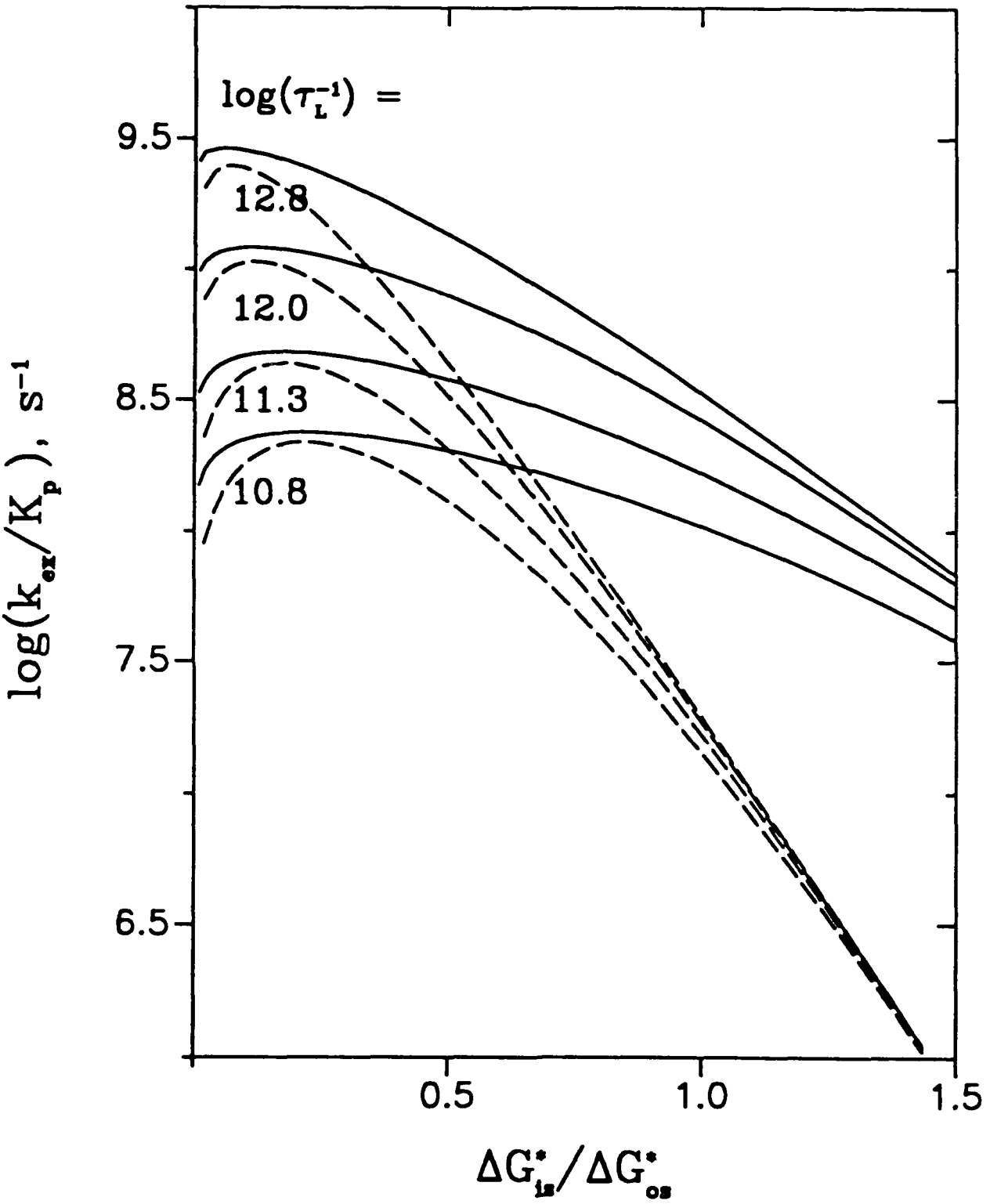
log(τ_L^-1) =
12.8
12.0
11.3
10.8
9.5
8.5
7.5
6.5
0.5
1.0
1.5
log(k_ex/K_p), s^-1
ΔG*_is/ΔG*_os

FIG 6